INL/JOU-14-32543
PREPRINT

THERMAL EVALUATION OF ALTERNATE SHIPPING CASK FOR IRRADIATED EXPERIMENTS

Nuclear Technology

Donna Post Guillen

June 2015

The INL is a
U.S. Department of Energy
National Laboratory
operated by
Battelle Energy Alliance

THERMAL EVALUATION OF ALTERNATE SHIPPING CASK FOR IRRADIATED EXPERIMENTS

Donna Post Guillen
Idaho National Laboratory
P.O. Box 1625, Idaho Falls, ID 83415
Donna.Guillen@inl.gov

ABSTRACT

Results of a thermal evaluation are provided for a new shipping cask under consideration for transporting irradiated experiments between the test reactor and post-irradiation examination (PIE) facilities. Most of the experiments will be irradiated in the Advanced Test Reactor (ATR) at Idaho National Laboratory (INL), then later shipped to the Hot Fuel Examination Facility (HFEF) located at the Materials and Fuels Complex for PIE. To date, the General Electric (GE)-2000 cask has been used to transport experiment payloads between these facilities. However, the availability of the GE-2000 cask to support future experiment shipping is uncertain. In addition, the internal cavity of the GE-2000 cask is too short to accommodate shipping the larger payloads. Therefore, an alternate shipping capability is being pursued. The Battelle Energy Alliance, LLC, Research Reactor (BRR) cask has been determined to be the best alternative to the GE-2000 cask. An evaluation of the thermal performance of the BRR cask is necessary before proceeding with fabrication of the newly designed cask hardware and the development of handling, shipping and transport procedures. This paper presents the results of the thermal evaluation of the BRR cask loaded with a representative set of fueled and non-fueled payloads. When analyzed with identical payloads, experiment temperatures were found to be lower with

the BRR cask than with the GE-2000 cask. From a thermal standpoint, the BRR cask was found to be a suitable alternate to the GE-2000 cask for shipping irradiated experiment payloads.

KEYWORDS

Thermal analysis; shipping cask; vacuum drying

I. INTRODUCTION

The Global Threat Reduction Initiative (GTRI) has many experiments yet to be irradiated in support of the High Performance Research Reactor fuels development program. The GTRI experiments are in the form of mini-plate capsules, full plates and elements [1]. Most of the experiments will be irradiated in the Advanced Test Reactor (ATR) at Idaho National Laboratory (INL), then later shipped to the INL Hot Fuel Examination Facility (HFEF) located at the Materials and Fuels Complex (MFC) for post irradiation examination. The ATR Complex is located approximately 32 km (20 miles) from MFC. Currently, materials are transported on a public highway either in full compliance with Department of Transportation (DOT) regulations or in "out-of-commerce" shipments when full compliance with DOT regulations cannot be achieved [2]. The General Electric (GE)-2000 cask is currently qualified for use at the ATR and HFEF facilities and has been used to transport GTRI experiments between them. However, the availability of the GE-2000 cask to support future experiment shipping is uncertain. It is not certain that GE will re-certify the liner and lid [3]. The current GE-2000 liner lid does not fit

properly and hasn't been previously used for shipping experiment payloads at INL. If the GE-2000 cask liner is no longer available, the required cool-down times prior to shipment may be excessively long. Also, the internal cavity of the GE-2000 cask is too short to accommodate shipping the larger GTRI experiment payloads as shown in Figure 1. These factors may make continued shipments with the GE-2000 cask impractical.

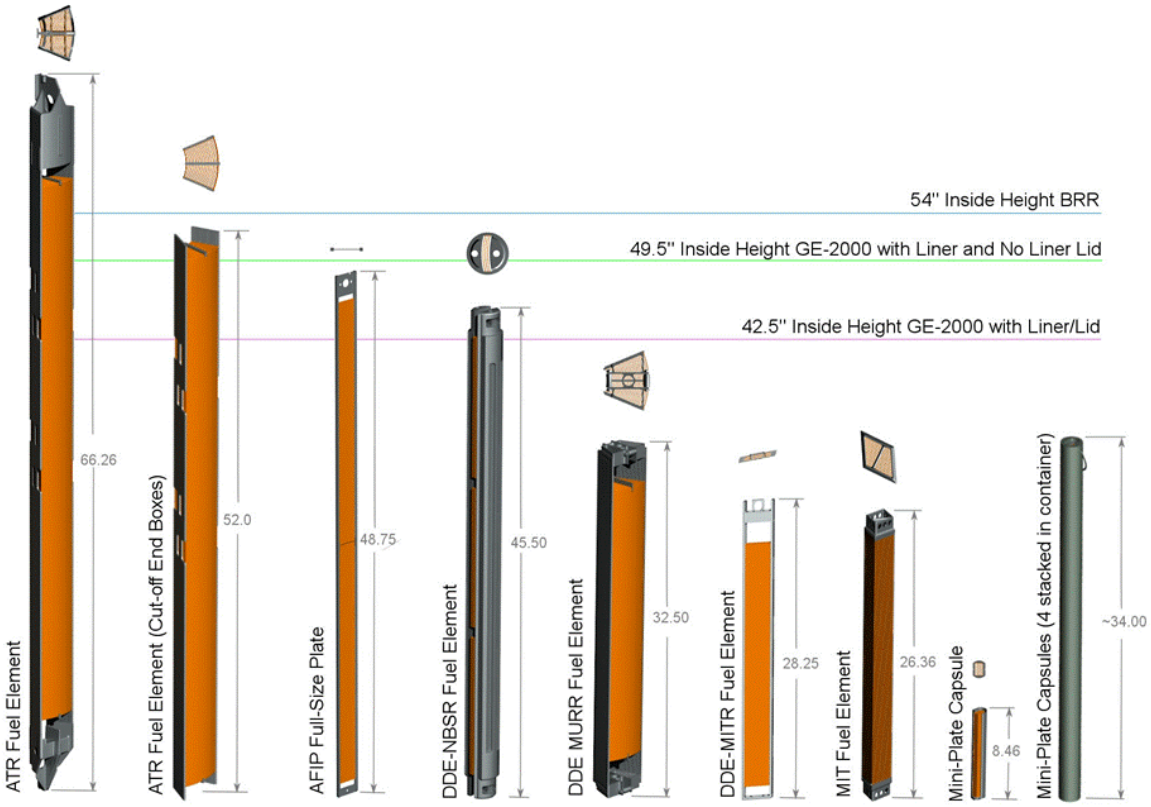

Figure 1. Heights of various GTRI Experiment Payloads [1].

The Battelle Energy Alliance, LLC, Research Reactor (BRR) cask has been determined to be the best alternative to the GE-2000 cask. Both the GE-2000 and BRR casks have a cylindrical internal volume, but have different dimensions for the height, volume, weight, and shielding. Both casks are constructed of stainless steel and require lead for radiation shielding. The

geometrical features of the BRR cask are compared to those for the GE-2000 cask in Table I. As can be seen in the table, the inside diameter of the BRR cask is smaller than the GE-2000 and the internal volume of the BRR cask is less than the volume of the GE-2000 (with or without the liner). The GE-2000 with the liner adds additional shielding, but also significantly reduces the overall payload capacity of the cask. The BRR cask has a taller internal cavity, which can accommodate the longer payloads and the built-in shielding is comparable to that of a GE-2000 with a supplemental lead liner.

Table I. Comparison of BRR and GE-2000 shipping cask dimensions [1].

	GE-2000 Cask	GE-2000 Cask w/ Liner	BRR Cask
Interior Height (m)	1.372	1.080	1.372
Interior Diameter (m)	0.673	0.514	0.406
Wall: Lead Thickness (m)	0.102	0.159	0.203
Wall: Steel Thickness (m)	0.051	0.070	0.081
Base: Lead Thickness (m)	0.000	0.057	0.196
Base: Steel Thickness (m)	0.152	0.171	0.053
Top: Lead Thickness (m)	0.140	0.267	0.246
Top: Steel Thickness (m)	0.076	0.095	0.089
Internal Volume (m^3)	0.488	0.224	0.178

Thermal limitations for shipping spent fuel are given in the Code of Federal Regulations (CFR) Title 49, Section 173.442 [4]. The external temperature of the BRR cask must not exceed 50°C due to the decay heat from the loaded payloads. In addition, to meet programmatic objectives and keep the experiment payloads from being damaged by excessive heat, the maximum experiment temperature must not exceed the threshold temperature determined by experimenters.

The purpose of this analysis is to determine whether the BRR cask is a suitable alternate to the GE-2000 cask from an experiment shipping standpoint. This paper presents the results of a thermal evaluation for the BRR shipping cask loaded with selected fueled experiment capsules and a representative ATR National Scientific User Facility (NSUF) non-fueled experiment. The payloads inserted into the cask for this analysis are part of an evaluation of the cask for a "typical" ATR experiment and not for a planned shipment, since these capsules have already been shipped. Rather, this analysis serves as a baseline to compare the thermal performance of the BRR shipping cask to the GE-2000 shipping cask with identical payloads. The same modeling approach was used – only the cask geometries are different. Before shipping any particular set of payloads, a thermal analysis with the actual loading configuration must be performed. A fully 3D model was built for this analysis so that it could be easily modified and adapted to incorporate other payloads. The model, analysis details and results are discussed in the following sections.

II. MODELING INFORMATION

The cask and associated components are designed to safely transport irradiated experiments from the ATR complex to the HFEF hot cell for post irradiation examination. In order to use the BRR cask at the INL, ancillary pieces of equipment were designed or modified to adapt to the BRR cask geometry. Figure 2 shows the overall dimensions of the cask, with the respective thicknesses of the stainless steel and lead shielding, along with an illustration of the

cask insert that was custom designed for this application. The BRR cask has built-in lead shielding and therefore does not require a supplemental lead liner.

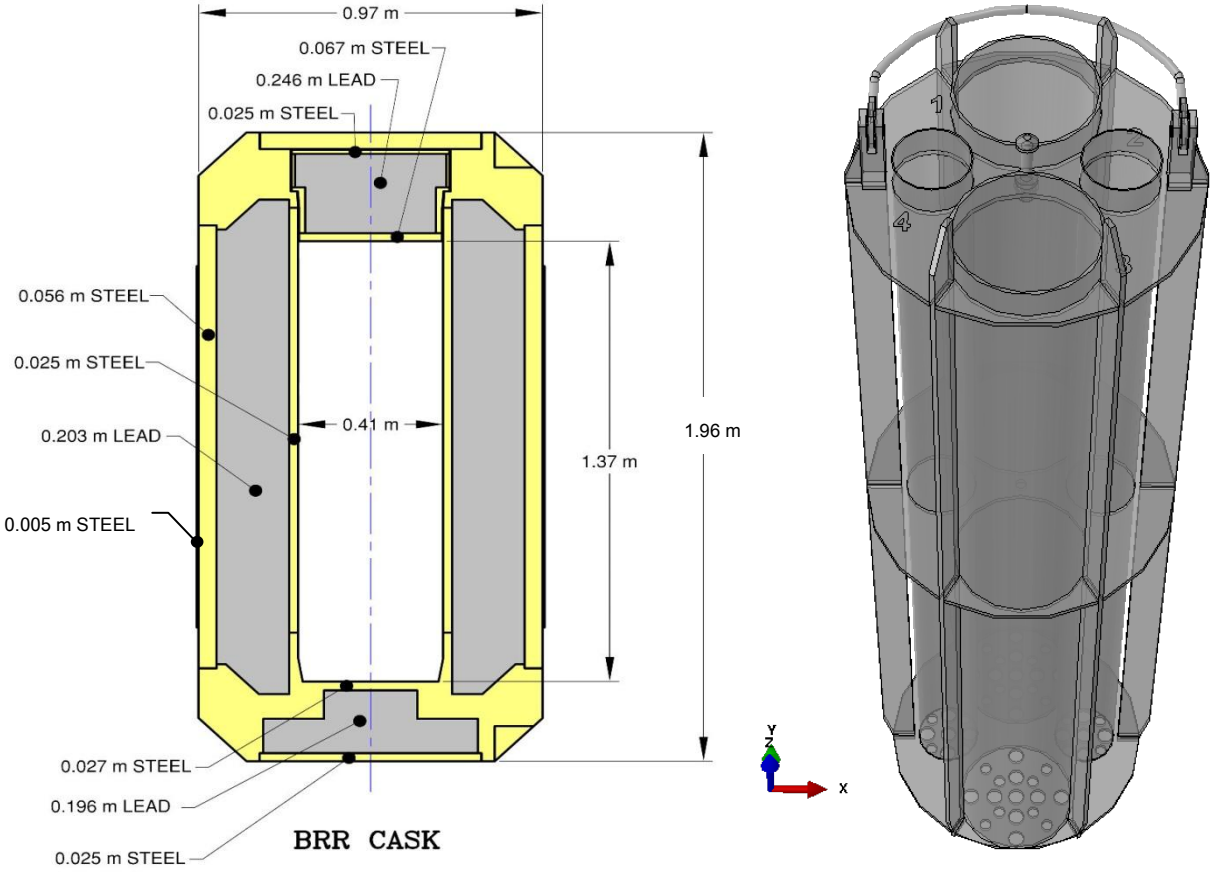

(a) (b)

Figure 2. (a) BRR shipping cask (cross-section view), (b) custom designed cask insert.

An aluminum alloy insert with four positions for payloads has been designed for use with the BRR cask. There are two large tubes (0.1615 m ID) and two small tubes (0.0856 m ID) that are 1.28 m long to hold irradiated payloads. The configuration analyzed includes five fueled capsules, along with various non-fueled NSUF experiment capsules. The five fueled experiment

capsules occupy two of the four cask insert positions. Two capsules are stacked axially in one position and the other three capsules are stacked in another position. The capsules are placed inside baskets that fit into the insert. The capsules are stacked one on top of the other to distribute the heat load along the basket length. Three capsules are located in one insert position, and two capsules are located in another position. This analysis conservatively assumes that the fueled capsules are located in the large tube positions in the insert, which provides a larger gas gap than the smaller insert positions. Each capsule is 0.2 m long and has a maximum width of 0.0328 m. The NSUF payloads are 0.0254 m in diameter and occupy the full length of one of the small insert positions. It is unimportant to the analysis which of the two remaining positions is occupied by the NSUF payloads. The NSUF payloads are placed within a basket inside of an insert tube.

A finite element model was developed to determine the maximum temperatures during shipping. The modeled assembly includes the cask, cask insert, baskets, position tubes and experiment payloads. The assembly was modeled using ABAQUS CAE [5] for construction of the finite element model and ABAQUS Standard to calculate steady-state temperatures and heat fluxes. This software has been validated using a standard set of textbook problems [6]. The finite element model geometry was constructed using three-dimensional solid elements using eight-node linear heat transfer bricks. The model contains approximately 338,000 elements. A structured hexagonal mesh was used wherever possible; in the remaining regions, a swept hex-dominated mesh was used. Mesh quality was enforced by verifying that the face corner angles, θ, of all elements met the criteria $45° \leq \theta \leq 135°$. A

mesh sensitivity study was performed by doubling the number of elements in each direction, with identical results.

Figure 3 shows a cutaway view of the entire model. Figure 4 shows a view from the top of the cask loaded with the insert and payloads. In the figure, the capsules are loaded in the large insert positions. The rod in the small insert position of Figure 4 represents the NSUF payloads. The fourth insert position, located at the left, is empty. The spacer plates used for positioning of the capsules are not modeled. Instead, they are represented by a simple position tube centered in the basket. This is conservative, since it increases the distance across the gas gap through which the heat must be transferred. The cask lid is not modeled since its effect on the heat transfer analysis is minimal. The predominant mode of heat transfer is radial conduction through the sides of the cask. The drain holes in the cask insert lower support plate (shown at the bottom of the cask insert in Figure 4b) are not modeled; rather, the lower support plate is modeled as a solid plate. There is a 0.005 m thick stainless steel thermal shield permanently affixed to the circumference of the cask body.

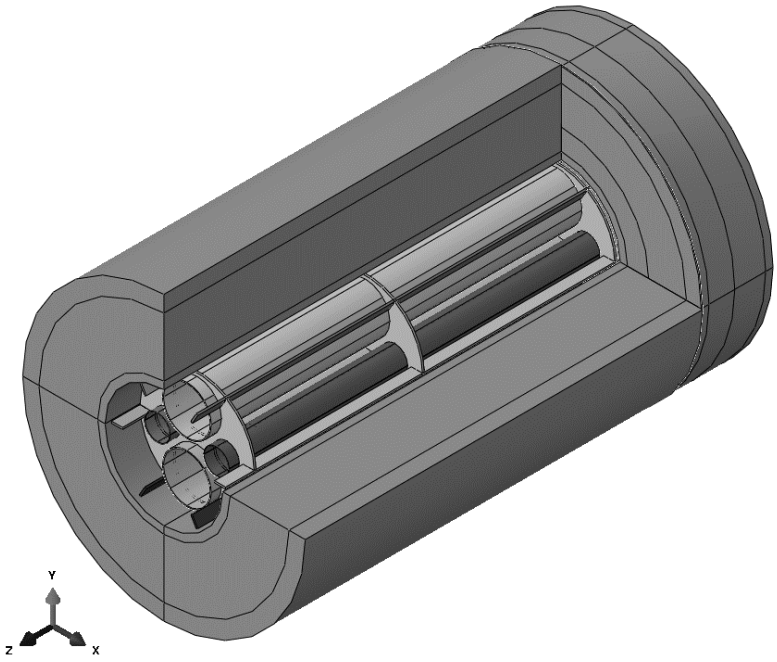

Figure 3. Cutaway view of BRR cask with insert loaded.

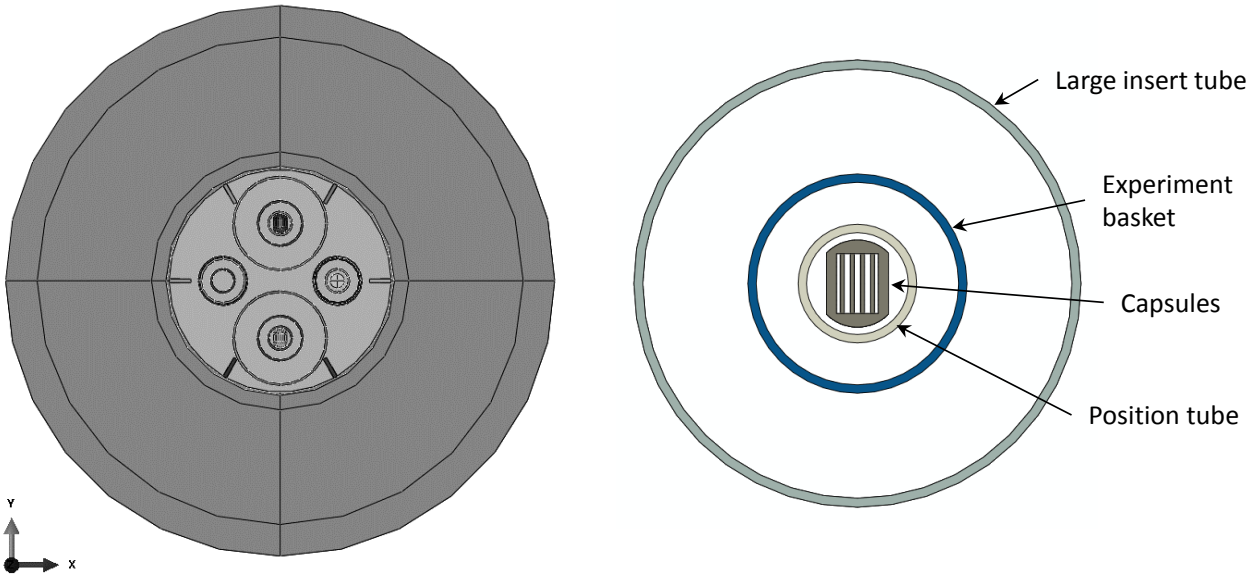

(a) (b)

Figure 4. (a) Top view of cask with payloads loaded, and (b) enlarged image of large insert tube with fueled experiment capsules, basket and position tube.

II. CALCULATIONS AND ANALYSIS

The most likely time for the cask and/or its contents to exceed temperature limits is during drying operations, when the cover gas pressure is reduced below the vapor pressure of water at the drying temperature [7]. Hence, the most adverse condition for heat transfer occurs during the vacuum drying process due to the reduction of the thermal conductivity of air at low pressure [8]. This can been seen from the results of an analysis of a spent fuel cask comparing the peak clad temperatures for vacuum, nitrogen and helium backfill where the highest temperatures occur for the vacuum backfill [9]. During the vacuum drying process, a low pressure (3 Torr) must be maintained for 30 minutes [10] to remove residual water that could deteriorate the materials or lead to a flammable condition caused by the radiolysis of water to free oxygen and hydrogen [11]. This analysis conservatively bounds the requirement by using the thermal conductivity of air at 0.5 Torr in a steady-state calculation.

As the gas pressure is reduced, there are less air molecules in a given volume. The mean free path of the gas molecules, λ (m), for an ideal gas is related to the temperature, T (K), and pressure, p (Pa), by the following equation [7]

$$\lambda = \frac{kT}{\sqrt{2}\pi p d^2} \tag{1}$$

where k is Boltzmann's constant (1.38×10^{-23} J/K) and d is the Lennard-Jones collision diameter for air (0.364 nm [12]). The mean free path for air at a pressure of 0.5 torr and temperature of

250°C is 2 x 10^{-4} m. From Equation 1, it can be seen that the mean free path increases as temperature increases and pressure decreases from standard conditions (typically given as 67 nm [13]). As a result, the heat transfer decreases due to the less frequent intermolecular collisions between gas molecules and the heated surfaces, which affect the energy exchange [14]. The degree of rarefaction of the gas is characterized by the Knudsen number, Kn, given by [7]

$$Kn = \frac{\lambda}{L_c} \tag{2}$$

where Kn < 0.01 for continuum flow, 0.01 ≤ Kn ≤ 0.1 for slip flow, 0.1 ≤ Kn ≤ 10 for transition flow, and Kn > 10 for free molecular flow. In Equation 2, L_c (m) is the characteristic length (in this case, the gap width, δ). The reduced pressure, coupled with the small gap sizes, within the shipping cask causes the validity of the continuum assumption to break down. For the BRR cask assembly, the gap sizes are such that the conditions are in the slip flow (for δ > 2 mm) or (for δ > 2 cm) continuum regime. For slip flow, the gas is rarefied to the extent that there is a temperature jump between the surface and the gas that acts as a thermal resistance. It is referred to as slip flow due to the velocity difference between the gas molecules and the surface [15].

At low pressure, the thermal conductivity of air varies with pressure, as well as temperature [16]. A curve fit for air at reduced pressure in thin gaps given in the General Electric Fluid Flow Handbook [17] was used to calculate the reduced thermal conductivity, k_r (W/m-K), of air during vacuum drying

$$\frac{k_r}{k_0} = \frac{1}{1 + 7.657 \times 10^{-5} \frac{T}{p\delta}} \tag{3}$$

where k_0 is the thermal conductivity at atmospheric pressure (W/m-K), p is the reduced (i.e., vacuum) pressure (Pa), δ is the gap size (m) and T is the absolute temperature (K). The coefficient in the denominator is a constant equal to 7.657 x 10^{-5} N/m·K, which has been converted to SI units from the British units originally given in [17]. This equation is applicable for the slip flow regime. As the pressure increases towards atmospheric, the right hand side of the correlation approaches a value of one. Equation 3 was applied for all of the gaps in the finite-element model. For gaps large enough to be in the continuum regime, the thermal conductivity used in the analysis is conservative.

For the case under consideration here, the environment within the cask consists of air under vacuum drying conditions. Therefore, the reduced thermal conductivity is used to compute heat transfer. Heat transfer coefficients for conduction across gas gaps are calculated as a function of gap size and temperature-dependent thermal conductivity of the air at the vacuum drying conditions. Gap conductance for small annular gaps can be expressed as [18]

$$h_{gap} = \frac{k_r}{\delta} \tag{4}$$

Equation 4 implicitly assumes that the Nusselt number is equal to one and the mode of heat transfer is pure conduction [19]. Contact surfaces for gap conduction are the respective inside surfaces and outside surfaces of components participating in the heat transfer. Radiation heat transfer was also accounted for in the interior of the cask. Emissivity values of 0.75 [20] and 0.2 [21] were used for the stainless steel and aluminum surfaces, respectively.

The upper and lower impact limiters are not installed during vacuum drying and therefore were not included in the model. The top and bottom surfaces of adjacent capsules are in good thermal contact. The base of the cask in contact with the floor is assumed to be adiabatic. All experiment heating is transferred through the sides of the cask via natural circulation to the surrounding environment.

Vacuum drying is performed in the ATR canal area, which is a large open space with a high ceiling, so heat transfer to the surrounding air will occur mainly by natural convection. The cask exterior surface is cooled by natural convection (and, to a lesser extent, thermal radiation heat transfer) to ambient air at 38°C. Climatology data for Arco, Idaho shows a historic average high outdoor temperature of less than 30°C for the summer months [22]. Based upon the climate data and the CFR Part 49 requirement, the prescribed sink temperature is a reasonable bounding value. The cylindrical-shaped cask has a relatively large curvature. Therefore, it is appropriate to approximate the cask external surface as a vertical plate. The following correlation [19] is used to calculate the Nusselt number, Nu, for free convection

$$Nu = \left[0.825 + \frac{0.387\left(Ra^{\frac{1}{6}} \right)}{\left[1 + \left(\frac{0.492}{\mathrm{Pr}} \right)^{\frac{9}{16}} \right]^{\frac{4}{9}}} \right]^2 \tag{5}$$

where Ra is the Raleigh number and Pr is the Prandtl number evaluated at the air film temperature.

The Raleigh number, Ra, is given by [19]

$$Ra = \frac{g\beta H^3 \left(T - T_\infty\right)}{\upsilon\alpha} \tag{6}$$

In Equation 6, g is the gravitational acceleration (9.81 m/s^2), β is the volumetric thermal expansion coefficient, given as the inverse of film temperature (K^{-1}), H is the height of the cask (m), T_∞ is the ambient temperature (K), υ is the kinematic viscosity of air (m^2/s) and α is the thermal diffusivity of air (m^2/s). The free convection heat transfer coefficient, h_{outer}, is calculated from

$$h_{outer} = \frac{Nuk}{H} \tag{7}$$

Fluid properties for air are evaluated at the film temperature. Temperature-dependent material and fluid properties are used in the analysis [19,20,23].

Heat is generated within the cask by radioactive decay of the irradiated fuels and materials within the payloads. The fueled experiment decay heat loads are obtained from the nuclear physics analysis, which provides heating rates for the fuel plates in the five fueled capsules. The radiation from the fuel plates in the capsules will be distributed throughout the cask, but most will be absorbed in the lead shielding. The analysis is conservative in that all of the gamma energy remains in the lead and is turned into heat. This is modeled by a source term in the energy equation. The decay heat loads applied to the fuel plates is shown for all

five capsules in Figure 5. The contribution to the total heating from the alpha and beta radiation is much higher than for the gamma radiation.

The total heat load from all of the fuel plates is 49.4 W. The total heating generated by the capsules is 91.9 W. All decay heating not deposited in the fuel (~42.5 W) is deposited in the lead portion of the cask. A uniform heat generation rate of 25 W is applied to the rod representing the NSUF payloads.

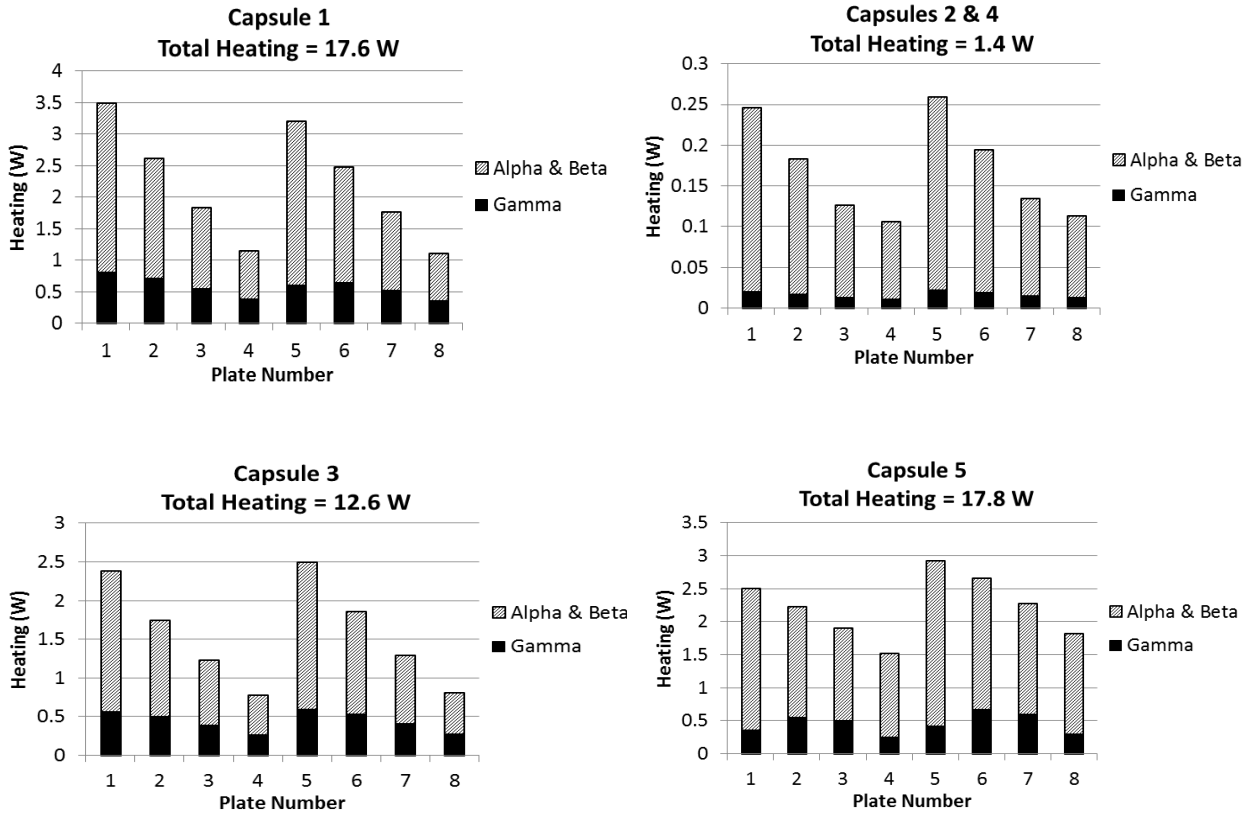

Figure 5. Fueled capsule heat loads.

IV. RESULTS AND DISCUSSION

Figures 6 through 9 show the results of the thermal analysis. The thermal load was evaluated under steady-state vacuum drying conditions. Figure 6 shows a cutaway view of the temperature distribution in the lead shielding. The lead shielding remains below the melting temperature of 327^{o}C [24]. The maximum lead temperature (43.3°C) occurs in the cask base. The heat is concentrated towards the base of the cask, since the fueled payloads are situated in the lower half of the cask.

Figure 7 shows a cutaway view of the temperature distribution in the entire cask. The gaps surrounding the payloads within the insert positions inhibit heat transfer through the cask during vacuum drying operations. The results of the analysis show that by incorporating the thermal shield, the maximum temperature of the payloads is lowered by slightly over 1.1°C. This is due to the competing heat transfer effects associated with an increase in cask thickness. The increase in external surface area decreases the convection resistance by more than the increase in thickness increases the conduction resistance.

The predicted maximum component temperature of 254.5^{o}C occurs in Capsule 1. This can be explained by referring back to Figure 5, which shows that Capsule 1 has the highest decay heat load. The maximum cask surface temperature of 47^{o}C occurs in the stainless steel base. The maximum temperature of the cask exterior surface is 42.3^{o}C. Figure 8 shows the temperature distribution along the mid-planes of the fueled capsules. As already noted, the highest temperature occurs in Capsule 1 since it has the highest heat load. Capsules 2 and 4 are the

coolest capsules since they have the lowest decay heat loads. The average temperature of Capsule 4 is nearly 100 °C lower than the peak temperature of Capsule 1. Figure 9 shows the temperature distribution in the NSUF capsules, which extend the full height of the position tube. The maximum temperature of the non-fueled NSUF rod (135.2°C) occurs in the lower half of the rod due to the heating from the surrounding capsule payloads. By comparison, the computed maximum experiment and external surface temperatures are 269.8°C and 56.3°C, respectively, for an equivalent experiment configuration loaded in the GE-2000 cask.

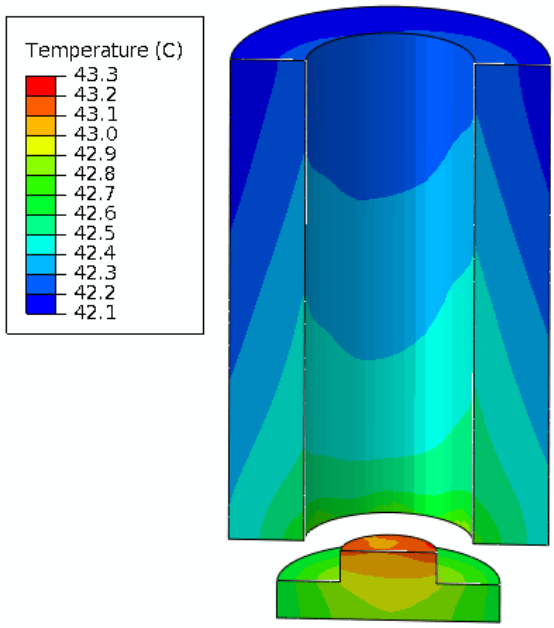

Figure 6. Cutaway view of cask showing temperature distribution in stainless steel structure and lead shielding.

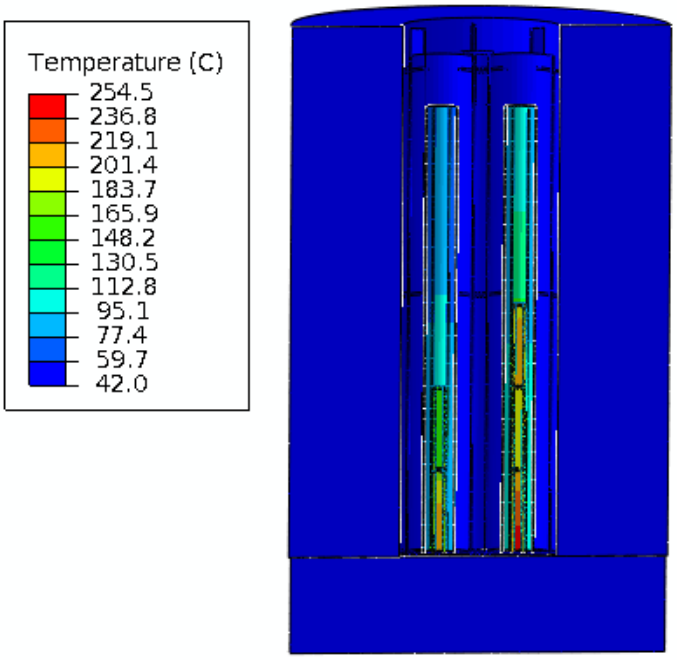

Figure 7. Cutaway view of temperature distribution (^{o}C) in entire BRR cask assembly.

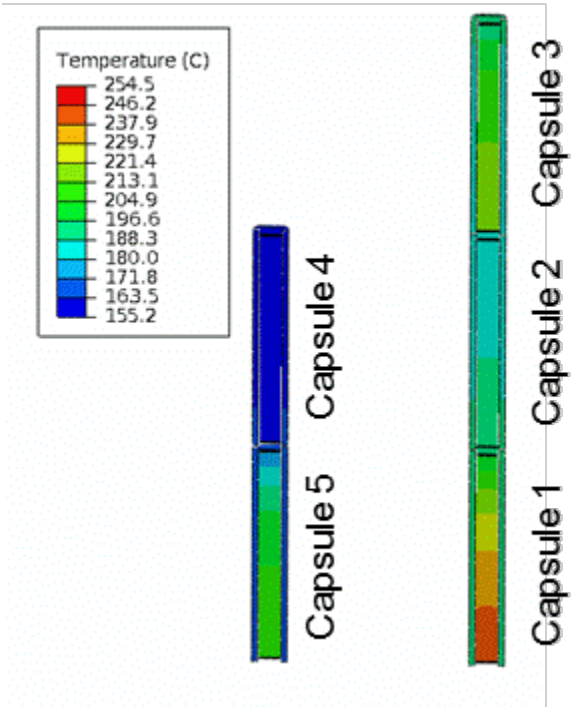

Figure 8. Temperature distribution (^{o}C) in the fueled capsules.

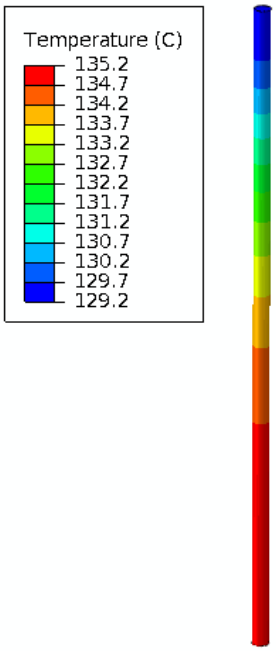

Figure 9. Temperature distribution (^{o}C) in NSUF capsules.

V. SUMMARY AND CONCLUSIONS

Results of a thermal evaluation are provided for a new shipping cask under consideration for transporting irradiated experiments between the test reactor and PIE facilities. A finite-element analysis was performed to evaluate the thermal performance of the BRR shipping cask loaded with typical irradiated fueled and non-fueled experiment payloads. The thermal load was evaluated for vacuum drying conditions, which is the limiting case for heat transfer from the payloads. The results show that the maximum temperature reached in any of the experiment capsules during vacuum drying is 254.5^{o}C. By comparison, the same set of payloads in the GE-2000 is predicted to reach 289.6^{o}C. The maximum temperatures of the BRR cask external surface and the lead shielding are within acceptable limits. Therefore, when loaded with an identical payload, the BRR shipping cask has been shown to perform as well or better than the

GE-2000 shipping cask. Therefore, from a thermal standpoint, the BRR cask is a suitable alternate to the GE-2000 cask for transporting irradiated experiment payloads. Before shipping any particular set of experiments, a thermal analysis with the actual loading configuration must be performed.

ACKNOWLEDGMENTS

This work was supported by the U.S. Department of Energy, Office of Nuclear Energy, under DOE Idaho Operations Office Contract DE-AC07-05ID14517. The author wishes to acknowledge Glenn Roth, who performed the thermal analysis for the GE-2000 cask and technical checking of the BRR cask analysis.

REFERENCES

1. J. BRYAN, “Evaluation of Cask Characteristics for GTRI Experiment Shipping,” Idaho National Laboratory Technical Evaluation (TEV), TEV-1737 (May 24, 2013).
2. “Environmental Assessment for the Multipurpose Haul Road within the Idaho National Laboratory Site,” U.S. Department of Energy, DOE/EA-1772 (August 2010).
3. Letter from Anthony E. McFadden, General Electric Vallecitos Nuclear Center, to Mark D. Lombard, U.S. Nuclear Regulatory Commission, AEM 13-08, July 1, 2013.
4. U.S. Department of Transportation, Code of Federal Regulations, Title 49, Section 173.442, Government Printing Office (2014).
5. Dassault Systèmes Simulia Corp., Providence, RI, USA (2013).
6. P. E. MURRAY, “Validation of ABAQUS Standard 6.7-3 Heat Transfer,” INL Engineering Calculations and Analysis Report (ECAR), ECAR-131 (January 2008).
7. D. COLMONT and P. ROBLIN, "Improved thermal modeling of SNF shipping cask drying process using analytical and statistical approaches," Packaging, Transport, Storage & Security of Radioactive Material, Vol. 19, No. 3, pp. 160-164 (2008).
8. J. LI, H. MURAKAMI, Y. LIU, P.E.A. GOMEZ, M. GUDIPATI, and M. GREINER, “Peak Cladding Temperature in a Spent Fuel Storage or Transportation Cask,” Proceedings of the 15th International Symposium on the Packaging and Transportation of Radioactive Materials, PATRAM 2007, Miami, Florida, October 21-26, 2007.
9. 22. J. M. CUTA, U. P. JENQUIN , and M. A. MCKINNON, “Evaluation of Effect of Fuel Assembly Loading Patterns on Thermal and Shielding Performance of a Spent Fuel

Storage/Transportation Cask," PNNL-13583, Pacific Northwest National Laboratory (November 2001).

10. Electric Power Research Institute, "High Burnup Dry Storage Cask Research and Development Project, Final Test Plan," Contract No.: DE-NE-0000593 (February 27, 2014).
11. U.S. Nuclear Regulatory Commission, "Standard Review Plan for Spent Fuel Dry Storage Systems at a General License Facility," NUREG–1536, Rev. 1 (July 2010).
12. A.S. FRIEDMAN, "Intermolecular Forces in Air," Journal of Research of the National Bureau of Standards, Vol. 58, No. 2, 93-94 (February 1957).
13. S.G. JENNINGS, "The Mean Free Path in Air," *J. Aerosol Sci.*, Vol. 19, No. 2, 159-166 (1988).
14. S. SONG, M.M. YOVANOVICH, and F.O GOODMAN, "Thermal Gap Conductance of Conforming Surfaces in Contact," Journal of Heat Transfer, Vol. 115, 533-540 (1993).
15. R. GREEN, E.T. MANZO, M. GREINER, J. LI, and Y.Y. LIU, "Experimental Benchmark of Simulations that Predict Temperatures of an 8x8 Array of Heater Rods within a Vessel Filled with Rarefied Helium Gas," Proc. 17th Inter. Symp. on Packaging and Transportation of Radioactive Materials, PATRAM 2013, San Francisco, CA, USA, August 18-23, 2013.
16. C.C. MINTER, "Effect of Pressure on the Thermal Conductivity of a Gas," U.S. Naval Research Laboratory, NRL Report 5907 (February 20, 1963).
17. General Electric, Fluid Flow Handbook, Genium Publishing, Section 410.2, May 1982.

18. K.J. GEELHOOD and W.G. LUSCHER, “FRAPCON-3.5: A Computer Code for the Calculation of Steady-State, Thermal-Mechanical Behavior of Oxide Fuel Rods for High Burnup,” NUREG/CR-7022, Vol. 1 Rev. 1, PNNL-19418, Vol. 1 Rev. 1 (May 2014).

19. F. P. INCROPERA, and D. P.DEWITT, *Fundamentals of Heat and Mass Transfer*, 5th Edition, John Wiley & Sons, New York (2002); also, 6th Edition (2007).

20. D. GREEN, and R. PERRY, *Perry's Chemical Engineers' Handbook*, Eighth Edition, McGraw-Hill (2007).

21. B. GEBHART, *Heat Transfer*, Second Edition, Literary Licensing, LLC (1961).

22. Western Regional Climate Center, Idaho Climate Summaries, http://www.wrcc.dri.edu/summary/climsmid.html, verified 02/05/2014.

23. J. FRANCL, W. D. KINGERY, "IV. Apparatus for Determining Thermal Conductivity by a Comparative Method, Data for Pb, Al_2O_3, BeO, and MgO," *J. Am. Ceram. Soc.* 37, 80-4 (1954).

24. *Marks' Standard Handbook for Mechanical Engineers*, 11th Edition, Table 4.2.28 Phase Transition and Other Data for the Elements (2007).